Journal of Spacecraft and Rockets

VOLUME 2 MAY-JUNE 1965 NUMBER 3

Progress on the Launch-Vehicle Buffeting Problem

A. Gerald Rainey
NASA Langley Research Center, Hampton, Va.

Nomenclature

C_A/C_{cr} = aerodynamic damping ratio to critical damping for bending oscillations
$C_{m_q} + C_{m_{\dot{\alpha}}}$ = aerodynamic damping coefficient for pitching oscillations
C_p = static pressure coefficient
D = reference diameter
f_m = model frequency
L = characteristic length
L_M/L = model length scale
M = Mach number
$P(\omega)$ = power spectrum, (pressure)^2-sec/rad
$(PSD)_M$ = power spectrum for model, (psi)^2-sec/cycle
$\overline{p^2}$ = mean square value of fluctuating pressure
q = freestream dynamic pressure
$R(\tau, x_1, x_2)$ = correlation function, normalized by $[R(0, x_1, x_1)-R(0, x_2, x_2)]^{1/2}$
V_c = convection speed
V_∞ = freestream velocity
α_M = amplitude of pitching oscillations, deg
Δx = $(x_2 - x_1)$
θ = phase angle between pressure at x_1 and pressure at x_2
τ = time lag
ω = rotational frequency, $2\pi f$

ABOUT four years ago, a series of launch-vehicle failures occurred during the transonic portion of their launch trajectories. The search for causes of these failures aroused an interest in the possibility that fluctuating pressures produced by separated flows and shock waves may have led to the failures. The buffeting phenomenon had not been considered in the design of these early vehicles in spite of the fact that buffeting has been a thorny problem in aeronautics for many years. This design "oversight" is quite understandable. Launch vehicles are generally long slender configurations in the over-all view. Four years ago it was not widely recognized that these slender shapes usually have local variations of cross-sectional area that are relatively rapid. These area variations lead to adverse pressure gradients and separated flow, which, in some cases, can cover extensive portions of the vehicle.

In addition to the highly dynamic buffeting phenomenon, these regions of separated flow can cause a variety of essentially static effects including stability and control problems and venting problems associated with rapid local static pressure drops. This paper, however, will be confined to the buffeting problem. A number of questions were raised when the possibility of buffeting on launch vehicles was recognized. What kind of aerodynamic flows are involved? How does this aerodynamic environment interact with the structure? A great deal has been learned regarding configuration features, which tend to alleviate the buffeting problem; however, it is seldom practical to compromise designs to the point where buffeting can be eliminated. Although this desirable goal should be kept in mind, generally it will be necessary to consider buffeting loads in the design of new vehicles or new payload shapes for existing boosters. Consequently, launch-vehicle design groups and research organizations are seeking answers to these questions. The intensive research that has taken place in the last four years is beginning to pay off, and it is considered appropriate at this time to survey progress toward answers to these questions.

The paper first considers what is known about the fundamental properties of the fluctuating pressures: their configuration dependency, basic dimensional behavior, and how well they can be generalized. The second part of the paper discusses the types of structural response to the aerodynamic input with emphasis on the state of the art of design procedures for buffeting.

Flow Phenomena

Configuration Effects

One of the well-established[1-7] characteristics of launch-vehicle buffeting is the fact that buffet pressures are very configuration-dependent. This configuration dependency is typical of most separated-flow problems and, consequently,

Mr. Rainey is head of the Aeroelasticity Branch of the Dynamic Loads Division. He has been engaged in conducting and supervising research on various aeroelastic problems since joining the staff of the Langley Research Center in 1946. Mr. Rainey has authored numerous publications in the fields of flutter and buffeting and served as a technical adviser to the U. S. Air Force on the Dyna Soar program. He is an Associate Fellow Member of the AIAA.

Presented at the AIAA Fifth Annual Structures and Materials Conference, Palm Springs, Calif., April 1–3, 1964 (no preprint number; published in bound volume of preprints of the meeting); revision received November 12, 1964.

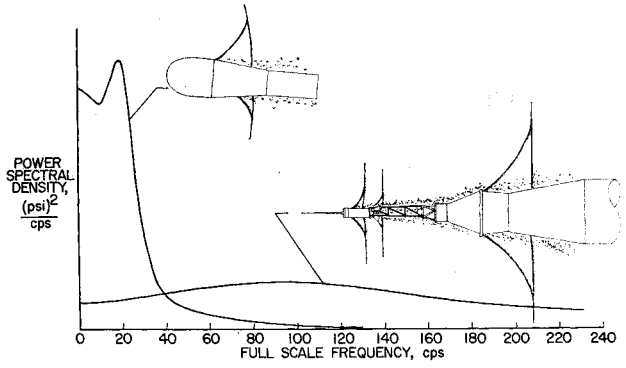

Fig. 1 Two types of buffet pressure spectra.

it is not surprising to find that buffet pressure intensity as well as frequency content is very much a function of the geometry producing the separated flow. The large variety of geometric configurations employed on launch vehicles leads to an almost equal number of types of buffeting flow. There are, fortunately, a few types of flow which can be discussed with some generality, and two of these are described in Fig. 1.

The power spectral density of fluctuating pressure at a point on two different configurations is shown in Fig. 1. The configurations selected for this illustration are the Atlas-Able V payload fairing[1] and the Mercury-Atlas vehicle.[5] It will be recalled that the power spectral density is a very useful property of a random process, and the fluctuating pressures that occur in buffeting are, indeed, random. The power spectral density provides a rough measure of the ability of a pressure to produce a structural response in a given frequency band. The curves indicate, for example, that the pressure acting on the Atlas-Able V shape would be relatively more effective in producing low-frequency bending response, whereas the Mercury-Atlas shape leads to pressures spread over a broad band of frequencies which would tend to be more effective in exciting high-frequency local responses. The point of the figure is that different configurations produce different types of flow, which, in turn, are characterized by pressure fluctuations having widely different frequency content. The Atlas-Able V shape produces a relatively simple type of shock-boundary-layer interaction with a highly localized region of fluctuating pressures near the foot of the normal shock wave. The Mercury-Atlas flow, however, can be described as a type of separated wake. Separated flow occurs well forward on the escape tower of this configuration and the remainder of the vehicle flies along in this wake.

These characteristics can be seen more clearly in Fig. 2, which shows schlieren photographs of the flow over portions of the Mercury-Atlas vehicle. These pictures were taken in the NASA Ames Research Center 9- by 7-ft supersonic wind tunnel. The Mach number in this case is 2.0, whereas the pressure spectrum of the previous figure was for a Mach number of 1.0; however, one of the interesting features of this separated wake type of flow is that the pressure fluctuations change relatively slowly with Mach number. Separation begins well forward on the escape rocket, and there is a clearly defined wake behind the rocket nozzles. The downstream portions of the vehicle are bathed in this wake, and fluctuating pressures occur virtually everywhere on the vehicle. There are numerous protuberances that produce their own wakes and, of course, there is a very complicated pattern of compression and expansion waves. The motion of shock waves induced by the wake turbulence undoubtedly contributes to the fluctuating pressures at a given point; however, this effect is probably spread over large areas because of the depth of the subsonic, highly turbulent wake surrounding the body. The high-speed flash used for these pictures has "frozen" a very interesting "chunk" of turbulence just over the adapter area. This "chunk" of turbulence has a height about equal to the local radius of the body, indicating a significant difference between this flow and a more conventional turbulent boundary layer that would exist on a cleaner configuration.

Another type of flow which has been observed for at least two configurations[6, 7] is illustrated by the schlieren photographs of Fig. 3. These pictures were made at the NASA Marshall Space Flight Center using a model of an early Saturn-Apollo configuration. The photographs illustrate a type of buffeting flow which has been termed "blunt-body separation." The point of interest in the figure is the flow at the front shoulder or the first cone-cylinder junction. Subsonically ($M = 0.9$) the flow cannot negotiate the abrupt change in angle and separates at the shoulder. Supersonically ($M = 1.1$) the boundary layer remains attached around this corner, indicating a gross change in the flow pattern over the vehicle. Actually, this change in flow pattern occurs in a much smaller increment of Mach number than the $M = 0.9$ to $M = 1.1$ range pictured in the figure.

As a matter of interest, two additional types of buffeting flow are visible in the upper portion of Fig. 3. At the nose of the vehicle, the previously discussed separated wake turbulence can be seen impinging on the nose cone. This model was equipped with a launch escape rocket; however, only the tower legs appear in the view shown. Toward the rear of the vehicle, a 45° conical frustum causes separation on the cylinder ahead of the frustum. Separation ahead of a blunt configuration feature is a relatively common occurrence.

There is a distinct change in local static pressures associated with the change from separated to attached flow and this feature is illustrated in Fig. 4. This figure[6] shows a plot of the usual static pressure coefficient at a point just behind the shoulder as a function of Mach number. Subsonically, the static pressure remains approximately constant up to a Mach number of about 0.93. At Mach numbers above 0.95, the flow is attached at the shoulder and there is a relatively abrupt drop in local pressures. This transonic static pressure drop occurs on almost all cone-cylinder configurations[8, 9]

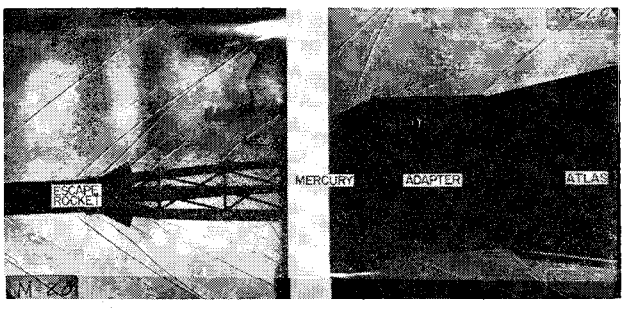

Fig. 2 Flow over the Mercury-Atlas vehicle.

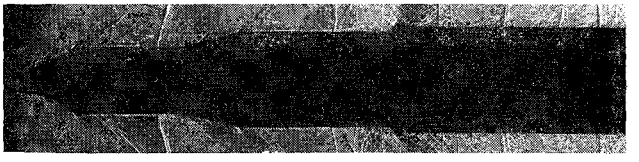

Supersonic, $M = 1.10$

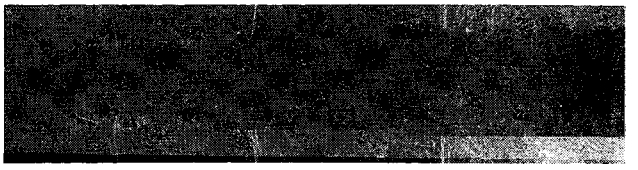

Subsonic $M = 0.90$

Fig. 3 Transonic flow on large launch vehicle.

and has led to failure of several launch vehicles. In the narrow range of Mach numbers where the jump occurs for the configuration of Fig. 4, the flow appears to be unstable and the pressures fluctuate randomly between the two levels representative of attached and separated flow. This leads to a time history of pressures resembling a random square wave as illustrated in Fig. 5.

The pair of time histories shown in Fig. 5[6] are for two models differing in size by a factor of 5. The models were of the configuration shown in Fig. 4 and the fluctuating pressures were measured at a station near the front shoulder. The square wave nature of the fluctuating pressure is a little more apparent in the lower figure for the smaller model. The tops of the wave tend to "bleed off" because the instrumentation system used did not have d.c. response.

Similar square wave pressure fluctuations have been observed by Kistler[10] for a portion of the separated flow ahead of a step at a Mach number of 3. Although the pressure fluctuations exhibit the same square wave characteristic, the relationship of the supersonic separated flow ahead of a step to the transonic flow around a cone-cylinder junction is not clear at this time.

The characteristic times of the random square wave are of some interest. A full-scale time increment of 1.5 sec has been indicated on the two time histories of Fig. 5. An increment of 1.5 sec has been selected for this discussion because that is the approximate length of time required for the vehicle to accelerate through the small range of Mach number where the square wave type of pressure fluctuation occurs. Examination of Fig. 5 indicates that the probability of encountering more than one of the large pressure jumps in a given 1.5-sec interval is relatively small. It would appear that, for this case, the treatment of the fluctuating pressures as a stationary random process would be an unjustified assumption. For the steady, fixed conditions of the wind-tunnel test, the fluctuating pressures have the required characteristics of a continuous random process; however, it seems likely that for the accelerating flight case the pressure would probably jump once from the subsonic, separated value to the supersonic, attached flow value. The relatively long characteristic time of these time histories is probably related to the relatively large dimensions of this configuration. The simulated full-scale diameter of the cylinder was 14 ft. A much smaller diameter blunt cone-cylinder configuration[7] indicated much shorter characteristic times and, consequently, the significance or interpretation of the wind-tunnel measurements with regard to vehicle response would be quite different. These considerations lead naturally to the question of scaling of buffet pressures which is discussed in the following section.

Scaling Considerations

The scaling relationships that have been applied to the analysis of launch-vehicle buffeting are based on simple dimensional considerations. These relationships are sometimes referred to as reduced-frequency concepts and they were originally proposed for the airplane buffeting problem by

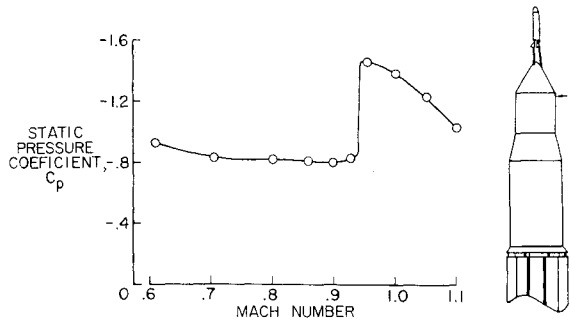

Fig. 4 Transonic static pressure drop.

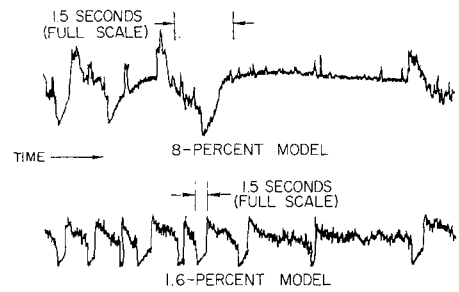

Fig. 5 Time histories of fluctuating pressure on manned lunar vehicle.

Liepmann.[11,12] Peterson and Ezra[13] have re-examined the application of these relationships to the launch-vehicle buffeting problem. Stated in its simplest form, these considerations lead to the result that the frequency of buffeting pressures should scale according to the reduced frequency $\omega D/V$ and the magnitude of the power spectral density can be expressed nondimensionally as $P(\omega)V/q^2D$.

There is good reason to question the validity of these scaling relationships. For example, it is seldom possible to conduct wind-tunnel tests at Reynolds numbers that equal the full-scale value and, consequently, the model boundary-layer characteristics will not exactly scale those of the full-scale vehicle. Similarly, surface roughness conditions are seldom scaled accurately on models. (Willmarth and Wooldridge[14] found an increase of about 50% of the fluctuating pressures due to a turbulent boundary layer on a machined surface compared to a smooth lapped surface.) Concern over the validity of these relationships has led to several evaluation studies. Jones and Foughner[6] have presented some results of this type, one example of which is shown in Fig. 6.

The upper portion of Fig. 6 shows the dimensional power spectrum of fluctuating pressure at a station on the configuration indicated in Fig. 4 obtained for two models differing in size by a factor of 5. The Mach number and Reynolds number were equal for the two tests and, since the models differed in size, there was a difference in the dynamic pressure for the two tests. The power spectra have been divided by the square of the dynamic pressure to make the otherwise raw test data somewhat comparable. The two sets of data form two distinctly different curves. In the lower portion of the figure, the data have been reduced to the nondimensional form mentioned previously, and it can be seen that the two curves approach very closely a single function of reduced frequency. This example is typical of other evaluations shown in Ref. 6; however, in all of these cases the Reynolds number was held constant for each comparison. A more comprehensive evaluation of the validity of wind-tunnel data

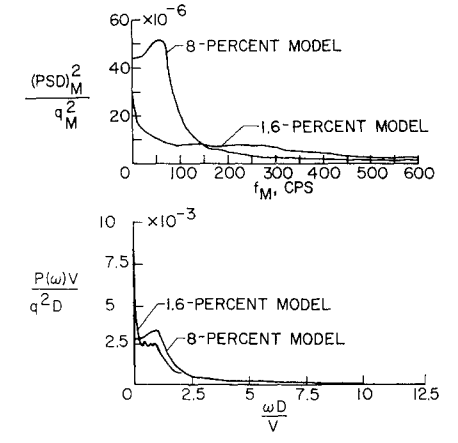

Fig. 6 Scaling of buffet pressure spectra.

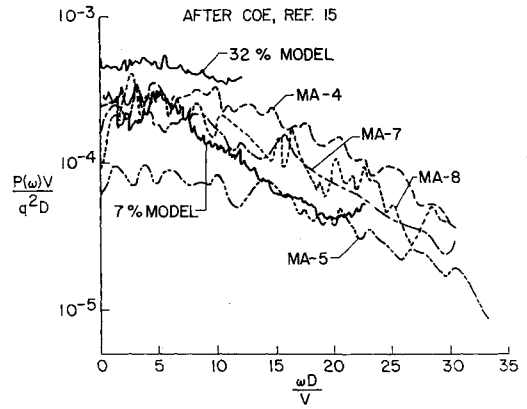

Fig. 7 Power spectra of pressure fluctuations on the Mercury-Atlas adapter near $M = 1$.[15]

would be to compare the model data directly with full-scale flight data. Coe[15] has recently presented comparisons of this type, some of which are discussed below.

Figure 7 shows the nondimensional power spectra of fluctuating pressures at a point on the adapter of the Mercury-Atlas vehicle. All of the data are for a Mach number near 1.0. The four sets of flight data* are for four flights of the Mercury-Atlas vehicle and they are compared with data from a 32% scale model test and a 7% scale model test. The 7% model data seem to approximate a reasonable average for the flight data. There is a considerable range in the different flight results and about the best that can be said for the 32% model data is that they agree with the highest level-flight data about as well as the highest flight data agree with the lowest flight measurement. Perhaps this figure may serve as an indication of the level of engineering accuracy that the current state of the art permits for the launch-vehicle buffeting problem.

Another comparison of model and full-scale results is shown in Fig. 8.[15, 16] In this case, the measurements are for a point downstream of the payload fairing on the Atlas-Agena-Ranger vehicle. The range of frequencies covered in this comparison is much more limited than in the previous case; however, over this range, the agreement between model and full-scale results is good. All of the comparisons discussed here were for model tests at reasonably high Reynolds numbers. As in other aerodynamic problems involving separated flow, buffeting pressures would be expected to be quite different at very low Reynolds number because the flow phenomenon is different. Data presented in Ref. 6 indicate a

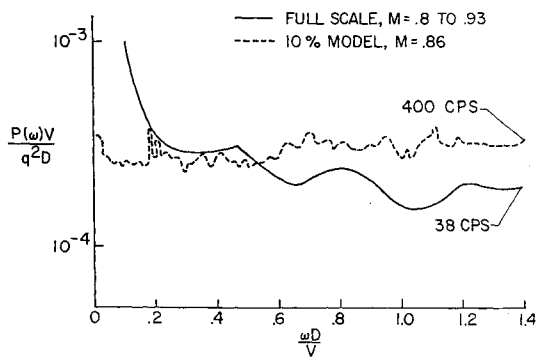

Fig. 8 Power spectra of differential pressure fluctuations on the Agena with the Ranger 5 payload.[15]

* The flight data have been compiled by James Ancell of the Aerospace Corporation.

marked effect of reducing the Reynolds number below the order of 10^6.

Coe presented another scaling comparison for another type of buffeting flow in which the reduced-frequency concepts did not properly correlate the data. This discrepancy is not readily explained. In spite of this case, examination of the many scaling evaluations that are available now indicates an over-all conclusion that the reduced-frequency concept is generally valid.

Generalized Characteristics

The fact that buffet pressures measured on small wind-tunnel models can generally be scaled to full-scale conditions successfully suggests that these pressures are dimensionally well behaved. If one could determine the proper characteristic dimensions to describe these pressures, then perhaps some common behavior might be found which would be useful in approaching the buffet load prediction problem. In view of the large number and complexity of the various flow phenomena discussed previously, the prospects of finding generalized characteristics must be considered to be small. However, the potential usefulness of results of this type is sufficiently great that an effort in this direction is justified. The results of one such attempt at correlating pressures from a variety of configurations is illustrated in Fig. 9.

The left-hand side of Fig. 9 shows the dimensional power spectral density of fluctuating pressure for several different configurations. Three of the four curves are model data scaled to full-scale conditions and the fourth is an average of the previously presented Mercury-Atlas flight data. Most of these data are for locations and test conditions which gave the highest levels of fluctuating pressure. It can be seen that the curves differ from each other by about two orders of magnitude in the ordinate and by about one order of magnitude in the abscissa.

In attempting to reduce data to a nondimensional form that might bring them closer to a single function, it was reasoned that the reduced frequency should be based on a characteristic length having something to do with the pressure-fluctuation-producing mechanism rather than an arbitrary dimension. Accordingly, for the Saturn-Apollo and Titan II, the diameter of the cone-cylinder junction where alternating flow occurred was selected as the characteristic length. Similarly, the maximum diameter of the bulbous payload fairing was selected for the Atlas-Able V and, somewhat arbitrarily, for the Mercury-Atlas, the maximum diameter of one of the escape rocket nozzles was chosen. In addition, the variations in intensity of pressure fluctuations due to the various configurations were removed by dividing the spectra by the mean square of pressure fluctuations $\overline{p^2}$ rather than by the dynamic pressure. The results of this reduction are shown in the right-hand side of Fig. 9. Reducing the data in this manner is sufficiently powerful to permit adding a spectrum of flat-plate turbulent-boundary-layer noise,[14] which would have been off the page if plotted dimensionally in the left-hand side of the figure. The characteristic length chosen for the flat plate was the displacement thickness of the boundary layer.

It can be seen that in this reduced form the curves differ from each other by less than an order of magnitude in both the ordinate and the abscissa. Admittedly, the generalized spectrum forms a rather "broad-brush" function that would require engineering judgment in selecting a characteristic length for application to other configurations. However, it seems striking that configurations involving flow phenomena with apparently large differences should yield data reducing to a nearly common characteristic. This result may prove useful in providing a preliminary design estimate of the "color" of buffeting pressures, and it is hoped that this result may provide a spark of inspiration leading to badly needed analytical advances in this field.

In addition to the frequency content and intensity, a complete description of buffeting pressure would include a description of its space-time correlation characteristics. Information of this type is necessary in applying the data in response calculations and would be extremely useful in obtaining a better understanding of the mechanism of production of fluctuating pressures. Data concerning the correlation characteristics of buffeting pressures are not available for a wide range of configurations and, consequently, it is not possible to determine whether or not these characteristics exhibit any common behavior patterns for various configurations. A few results of this type have recently become available from the measurements made on the Mercury-Atlas models, and some of the interesting aspects are summarized in Figs. 10 and 11.

Figure 10 shows a selection of correlation functions obtained for the 32% scale Mercury-Atlas model that was tested in the U. S. Air Force Arnold Center propulsion wind tunnel. The correlation coefficient is a gross measurement of the "togetherness" of two pressures. It is, of course, a function of how far apart the two pressure measurements are made (Δx), and by adjusting the time lag between the two signals τ an immediate impression can be had as to whether or not the pressures are being convected from the upstream point to the downstream point. This convection pattern is clearly indicated in Fig. 10 by the translation to the right of the positive peaks for the three shortest separation distances. Although the magnitude of the positive peaks indicates a fairly rapid decay of the correlation with distance, the occurrence of the peaks displaced in time suggests a picture of convected patterns of fluctuating pressure which decay as they move downstream. This behavior has been found to describe, generally, the pressures due to a subsonic turbulent boundary layer.[14] The convection speed for the Mercury-Atlas determined from the translation of positive peaks varies in the range from about 36 to 43% of the freestream velocity depending on the separation distance. This convection speed is considerably lower than that found for the subsonic boundary layer, which varied in the range from 56 to 83% of the freestream velocity.

The behavior of the negative peaks in the correlation curves of Fig. 10 is interesting. Contrary to the positive peaks, which decay exponentially with separation distance, the negative peaks appear to grow with increasing values of separation distance reaching a maximum value at distances of about 2 ft for the model. This behavior is not clearly understood, but it may be due to slowly convected large-scale eddies.

The correlation function describes the behavior of the entire pressure fluctuation spectrum lying within the frequency limitations of the measurement system. The Fourier

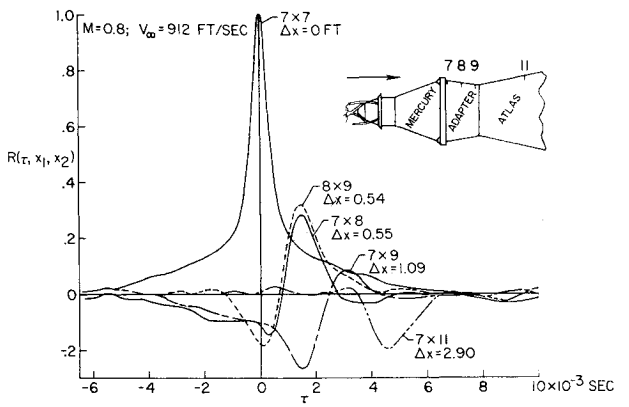

Fig. 10 Buffet pressure correlation functions for 0.32-scale Mercury-Atlas model.

transform of the correlation function is the cross-power spectrum, which permits deductions regarding the correlation characteristics in different parts of the frequency spectrum. The cross-power spectrum is, in general, complex, and for a convection phenomenon of the type involved in these buffeting flows, the phase angle determined by the real and imaginary parts of the cross spectrum can be interpreted as representing the time lag for the pressure acting at the upstream point to reach the downstream point. Of course, this phase angle can be determined for each frequency, and, consequently, the time lag can be determined as a function of frequency. Time lag as functions of frequency has been determined in this manner for several different cases on the 32 and 7% scale models of Mercury-Atlas, and the results are shown in Fig. 11. The time lags have been made nondimensional by use of the separation distance Δx and the freestream velocity V_∞. Again, the frequency is presented in reduced form using the arbitrarily chosen "characteristic length" of the escape rocket nozzle diameter.

It can be seen that all of the various cases tend to merge into a single function at reduced frequencies above about 0.4. This merging of the data is considered to be remarkable in view of the large range of parameters covered by the different cases particularly when it is recalled that the two different models were tested in two different wind tunnels using different instrumentation and data reduction methods. At a reduced frequency of 0.4, the average nondimensional time lag is about 2.8 and tends to decrease smoothly with increasing frequency to a value of about 1.9. Using the approximation $dx/d\tau \approx \Delta x/\Delta\tau$, it can be recognized that the nondimensional time lag is the reciprocal of the convection speed ratio

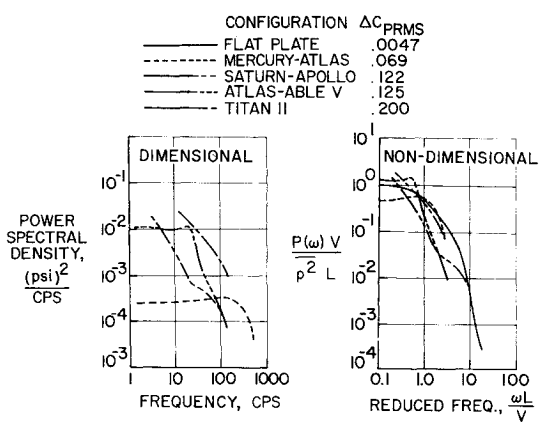

Fig. 9 Generalized spectrum of aerodynamically produced fluctuating pressures.

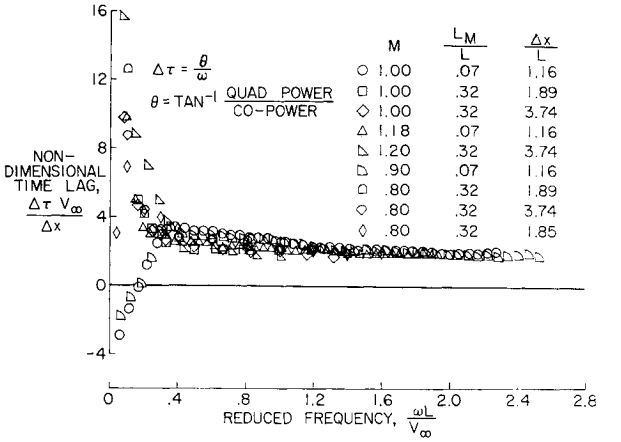

Fig. 11 Convection characteristics of buffet pressures on Mercury-Atlas adapter.

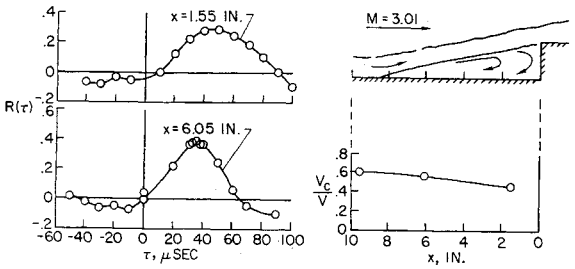

Fig. 12 Convection characteristics under a supersonic separated flow[10] (V = 25,000 in./sec, Δx = 0.5 in.).

$\Delta x/\Delta\tau V_\infty = V_c/V_\infty$. Therefore, the data in Fig. 11 indicate a variation of convection speed with frequency from about 36% at a reduced frequency of 0.4 to about 53% at reduced frequency of 2.5. Again, this increase of convection speed with frequency is contrary to results found for the subsonic flat-plate boundary layer.

The two branch curves formed by the data at reduced frequencies below 0.4 are not easily explained. The lower branch crosses the axis and becomes negative. This must mean that low-frequency pressures were propagating upstream. Nearly all of the transonic wind tunnels generate noise in their diffusers which propagates upstream. Although one set of negative points is for a Mach number of 1.0, it is possible that the noise could advance through the subsonic wake of the model-string arrangement. A more "desirable" explanation (for those of us who like to think that wind tunnels reproduce the flight environment) is that the low-frequency pressures are convected upstream by the reversed flow adjacent to the body underneath the separated boundary layer.

The upper branch of the data in Fig. 11 appears to be caused by slowly convected large-scale eddies, and it is this part of the spectrum which is probably responsible for the negative peaks in the correlation functions of Fig. 10.

Another study concerning correlation characteristics of buffeting pressures has been presented recently by Kistler[10] and his results are summarized in Fig. 12. The case considered here is the separated flow ahead of an abrupt step at a Mach number of 3.01. The flow picture is illustrated in the right-hand side of Fig. 12 and two cross-correlation functions for wall pressures measured within the separated-flow region are shown on the left. Again the pressures are convected downstream in spite of the definite reverse flow next to the wall. Of course, the correlation function gives an over-all measure of the convection picture, and cross spectra have not been presented which would allow an evaluation as to whether some parts of the pressure spectrum may be convected upstream. The convection velocity obtained from the correlation functions is plotted in the lower right-hand portion of the figure. The convection speed is highest in the attached supersonic boundary layer dropping off from about 60% of freestream velocity to about 44% toward the rear of the separated region.

Response Considerations

Up to this point, the paper has been concerned with the buffeting pressures and the flows that produce them. These pressures represent the input to the structural system and the designer wants to know how much output load, deflection, acceleration, or stress response the structure will be subjected to. In principle, once the input pressures are defined the calculation of response is relatively straightforward. However, as is often the case, practical difficulties lead to the need for simplifying assumptions and several different approaches have been developed. Perhaps these practical difficulties can be described more readily after examining an expression for the response. Houbolt[17] has developed rather simply an expression for the response which is repeated below. The spectrum of the response (in terms of any quantity linearly related to displacement) at a station y is

$$P_y(\omega) = P_1Z_1Z_1^* + P_2Z_2Z_2^* + P_3Z_3Z_3^* + \ldots + 2Re(P_{12}Z_1Z_2^* + P_{13}Z_1Z_3^* + \ldots + P_{23}Z_2Z_3^* + \ldots)$$

Where P_1 is the spectrum of input acting at station 1, P_{12} is the cross spectrum of input between station 1 and station 2, and Z_1 is the frequency-response function for the response at y to an input at station 1. The asterisk denotes the complex conjugate.

This equation is a general expression for the response of a distributed system to multiple random inputs. It contains a multiplicity of terms, some of which are very difficult to obtain either experimentally or analytically.

One of the most frequently employed simplifications is to treat the problem as though there were only a single input. This approach requires only the first term on the right-hand side and simplifies to

$$P_y(\omega) = P_1Z_1Z_1^* = P_1|Z_1|^2$$

which is the well-known input-output relationship for a linear lumped parameter system with a single input. This approach is seldom satisfactory because buffeting generally involves a distribution of input pressures. If the significance of multiple inputs is recognized, something must be done to account for the cross-spectrum terms. In some cases, the cross spectra have been accounted for by assuming that the pressures at stations 1 and 2 are completely correlated[5, 18–20] or that $P_{12}(\omega)$ is zero. Measurements of complete sets of cross spectra are sufficiently difficult and complicated that, for the transonic launch-vehicle buffeting case, they have appeared in the literature only within the last year.[21] In addition, the frequency-response functions Z are difficult to treat when we are concerned with high-frequency shell modes, for example. Fortunately, many investigators are studying several approaches for solutions of this problem and, in the following sections, an attempt will be made to present the current state of the art of the various methods of handling the response problem. The response problem, for discussion purposes, has been divided into two sections, concerned first with high-frequency local response and second with low-frequency bending response.

High-Frequency Local Response

The high-frequency local response problem has not received the attention that the low-frequency bending problem has attracted. Perhaps this is because the beam problem is easier to deal with. The reason does not lie in the relative severity of the two problems, because in those cases of vehicle failure or malfunction which have been traced to buffeting as a possible

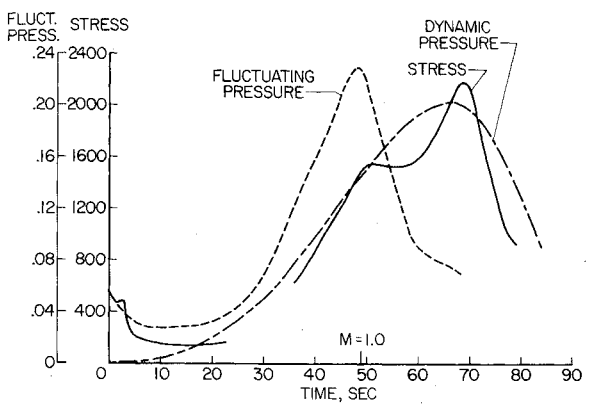

Fig. 13 Time histories of rms stress, rms pressure, and dynamic pressure for Mercury-Atlas-5.

cause, the high-frequency problem predominated. It seldom has been possible to pin down the nature of buffeting response in flight because very few launch-vehicle programs included a completely instrumented flight intended for measuring loads in flight. A few scattered flight results are available, and one set of these is described in the following section.

Flight measurements

One vehicle failure that was suspected of being due to buffeting was the first flight of Mercury-Atlas or MA-1. As is often the case, there were insufficient measurements made during the flight to settle the question as to what caused failure or as to exactly where the failure was initiated. The vehicle was beefed-up on a fairly arbitrary basis and no subsequent failures have occurred. The beef-up of the Mercury-Atlas adapter was intended to stiffen and strengthen that component of the structure to shell-mode-type vibrations. During the MA-5 flight, measurements of local fluctuating strains were made at two points on the adapter. One of these measurements was of the bending strains between the inner skin and outer cap of the corrugation-stiffened shell. The time history of root-mean-square fluctuating stress at this point on the adapter is shown in Fig. 13. As mentioned previously, the fluctuating pressure at a point on the adapter was also measured on MA-5, and these results, along with the freestream dynamic pressure, are also shown in Fig. 13 as a function of flight time. The fluctuating pressure, as predicted from wind-tunnel measurements, drops off at Mach numbers above 1.0 even though the dynamic pressure continues to increase. The fluctuating stresses continue to increase beyond $M = 1.0$ and tend to follow the peak and dropoff of freestream dynamic pressure. Although the stress levels are quite low for this beefed-up adapter, it is interesting to note that the fluctuating stresses do reach a maximum level at about the same time in the trajectory when failure occurred on the MA-1. The fact that the stresses in a structural component continue to rise while the fluctuating pressures producing the response are falling off is indicative that the phenomena of convected patterns of fluctuating pressure, which were discussed previously, must be accounted for if we are to make progress in predicting this type of response. The fall-off in pressure fluctuation with increasing stress is, of course, contrary to what would be expected for ordinary acoustic excitation by plane waves impinging normal to the surface. In fact, a full-scale test adapter has been subjected to a high-level acoustic environment and it was found that the stresses increased linearly with input pressure.

The frequency content of the fluctuating stresses and pressure are of interest and these are shown in Fig. 14 for a time corresponding to the $M = 1.0$ point in the trajectory. The pressure spectrum, which was presented earlier, is a relatively flat continuous curve. The stress spectrum, on the other hand, shows two distinct peaks at frequencies between 350 and 400. These frequencies correspond to modes that have been measured in a ground vibration survey; however, these modes have not yet been identified in the usual manner of identifying shell modes. That is, it cannot be stated that these modes had m longitudinal half-waves and n circumferential waves. The mode shapes and frequencies of practical shell structures are very difficult to measure. Energy dissipation around the shell and pairs of modes occurring at the same frequency sometimes distort the classical picture. The modes of maximum response in flight were determined to be the modes that were most easily excited (in terms of response of the strain gage) by single-point sinusoidal excitation and by acoustic excitation surrounding the structure.

The flight evidence and experience with a practical shell structure indicate that the high-frequency buffet response problem is not a simple one. Progress on research directed toward methods of handling this aspect of the buffet problem is discussed in the following sections.

Analytical approaches

The basic formulation of the high-frequency response problem is, of course, the general formulation discussed previously. This result has been available for many years. As is so often the case, however, practical design procedures employing this formulation have not been developed or evaluated to the point that routine calculations can be made.

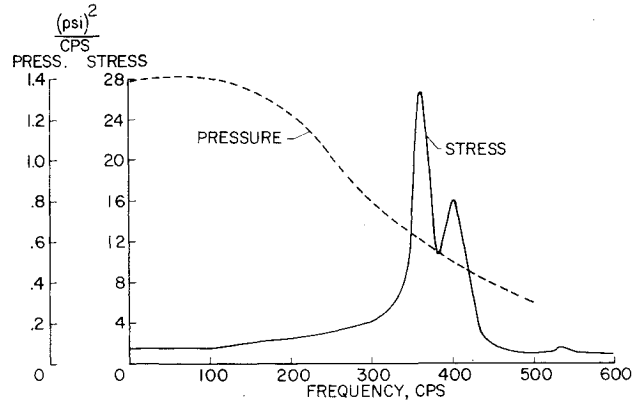

Fig. 14 Power spectra of stress and pressure for Mercury-Atlas-5 ($M = 1.0$).

The main areas of difficulty lie in the definition of the aerodynamic input and in the structural dynamics of the system. A research program is underway at the NASA Langley Research Center, which has as its limited goal the demonstration of the applicability of the basic response relations to the problem of a simplified rectangular flat plate responding to an acrodynamically produced fluctuating pressure. The experimental setup consists of a plate mounted on springs, which are made soft in the plane of the plate in an attempt to relieve midplane stress effects thus tending to linearize the structural behavior. The fluctuating pressures are generated by a spoiler mounted upstream of the test specimen. Inputs are measured by replacing the flexible panel with a heavy plate equipped with 12 pressure transducers. The effects of aerodynamic damping will be examined by measuring the damping of the modes with and without airflow. Preliminary testing has been completed; unfortunately, however, no useful results can be quoted at this time.

Even if this exercise in application of the response equation is successful, the problem of calculating response of practical structures to actual aerodynamic environments remains to be examined. The McDonnell Aircraft Company under contract to the NASA Langley Research Center is conducting research in this area. The ultimate objective of this research is to provide practical engineering methods of accounting for high-frequency buffet response of structural components in a rational manner during the design of new vehicles. The scope of the contract includes an examination of the aerodynamic input, study of methods of treating the structural characteristics, and combining the first two items to calculate the response. The methods developed will be evaluated by comparison of the results with the available full-scale data on the Mercury-Atlas adapter. As an example of the kind of work underway, a comparison of calculated and measured radial accelerations at a point on the adapter is shown in Fig. 15. The calculation was made using input data, extrapolated from 7% scale wind-tunnel model results, distributed over 80 elements (4 longitudinal by 20 circumferential increments). The structure was represented by 19 normal modes. Detailed comparison of the level and frequency of the various peaks in the spectra does not indicate very good agreement. However, comparison of the over-all root-mean-square acceleration

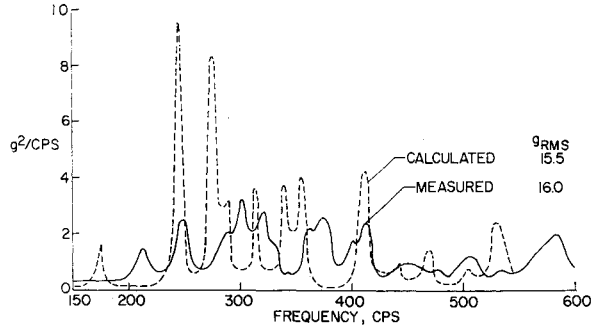

Fig. 15 Comparison of measured and calculated spectrum of radial acceleration on Mercury-Atlas adapter (MA-4 flight, $M = 2.0$).

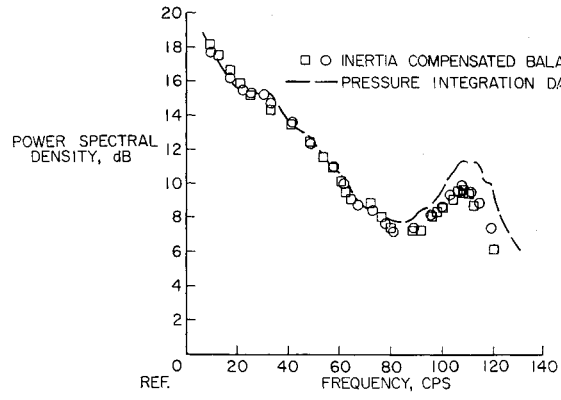

Fig. 17 Comparison of aerodynamic moment PSD.[26]

shows excellent agreement, a result that must be considered as fortuitous in view of the fact that these preliminary calculations do not incorporate several significant aspects of the problem. The McDonnell work is continuing toward finding those simplifications that will make the problem feasible for treatment but that will retain the essential physical characteristics.

Aeroelastic modeling techniques

One approach to the problem of predicting high-frequency local response of structural components is to subject a model of the structure to a suitable test environment. This approach has been successfully demonstrated[22,23] for the Snark missile, which had a severe acoustic environment associated with its jet-assisted takeoff (JATO) bottle booster rockets. A suitable test environment for buffeting response of a launch vehicle is provided by wind tunnels. Generally, requirements for a satisfactory aeroelastic model of a component of a launch vehicle leads to a replica-type model where each significant structural element is made of prototype material and simply scaled down in size. Of course, compromises must be made; rivet patterns cannot be scaled exactly, for example. In addition, launch-vehicle structures grow larger each fiscal year and wind tunnels suitable for generating buffeting inputs remain the same size. This leads to a need for research to determine the practicality of building replica-type models small enough to be tested in an aerodynamic environment yet with sufficient detail to provide accurate simulation of high-frequency shell modes. A research program having this objective is underway at the NASA Langley Research Center. The Apollo vehicle is expected to encounter a relatively severe buffeting environment during launch. Accordingly, the first boiler-plate development vehicles will be relatively well instrumented for buffet input and response. Because the flight data will be

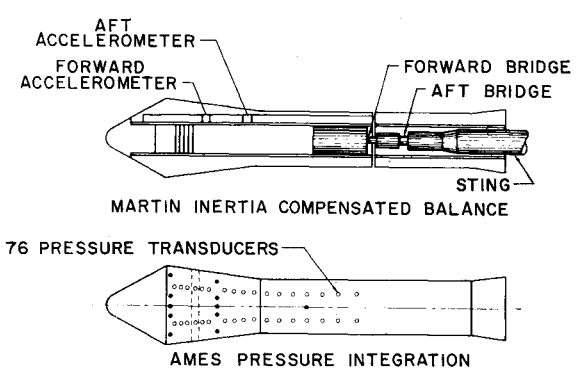

Fig. 16 Comparison of ICB instrumentation and pressure integration instrumentation.[26]

available, this vehicle has been selected for an attempt at simulation of the high-frequency buffet response in a wind-tunnel test. The component that has been selected for modeling is the Apollo boiler-plate service module. A $\frac{1}{10}$ scale model is in fabrication. The model will contain structural elements as thin as 0.008 in. thick. There are about 2000 separate parts, which will be fastened together by about 28,000 rivets. The model rivet size is such that for every three full-scale rivets there will be only two model rivets. The proper aerodynamic environment will be generated by conventional rigid components of the forward and aft portions of the launch configuration. It is estimated that about 5500 man-hours will be required for fabrication of the complete model.

The state of the art that has been presented for the high-frequency buffeting response problem indicates a picture of developing techniques. The approaches and methods for handling the problem exist, but they require further development and evaluation before it can be said that the problem is well in hand. Fortunately, a concerted effort is underway which should soon provide the technology required to make the various approaches suitable for general application in design. The state of the art for the low-frequency bending response problem is in considerably better shape and that picture is developed in the following section.

Low-Frequency Bending Response

Analytical approaches

Analytical methods, for purposes of this discussion, are arbitrarily defined as approaches involving a basically analytical treatment of the equations of motion of the structural system as opposed to a mechanical analog treatment, which is discussed subsequently. In addition to the previously referred work[5, 18–20] another promising analytical approach has been developed at the Martin Company.[24]

This approach involves the use of a special type of strain-gage balance system for measuring the input required in

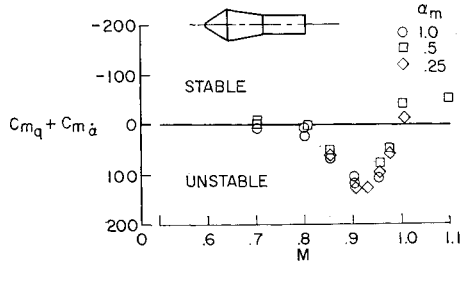

Fig. 18 Aerodynamic damping of a bulbous payload.[28]

solving the response problem. The special balance is one that includes properly located and calibrated accelerometers, which are used to correct the strain-gage signals for inertia loads produced by the buffeting forces. The balance is called an inertia compensated balance (ICB), and some of its features can be compared with a pressure-measurement technique in Fig. 16. The pressure-measurement technique indicated in Fig. 16 has been developed by the NASA Ames Research Center.[25] The basic simplification involved in both these approaches is to replace the measurement of a large number of individual inputs by one or two inputs in the form of moments about a selected axis. The pressure technique accomplishes this by electrically summing the outputs of a large number of pressure transducers. The ICB technique measures the total integrated moments, rejecting the very large inertia loads produced by small vibrations of the model on the balance.

The degree to which the two techniques give comparable results is illustrated in Fig. 17, which shows the power spectral density of integrated moments obtained by the two methods. The power spectra are plotted to a decibel scale with arbitrary reference. It can be seen that the two methods are in excellent agreement. The application of results of this type requires certain assumptions that are common to both methods. Obviously, the buffeting input is obtained only for that part of the vehicle which is simulated in the model program, and for some configurations it is not appropriate to assume that the only input is from the payload shape. Secondly, the application of the moment data requires the transformation of the translational or bending degrees of freedom into equivalent rotational degrees of freedom. This can sometimes lead to uncertainties when the mode shape of the simulated portion of the model deviates appreciably from a straight-line approximation. Thirdly, both techniques require another model test or analysis to provide an estimate of the aerodynamic damping for the full-scale vehicle. Techniques that have been developed to eliminate the need for some of these assumptions are described below.

Dynamic modeling techniques

Cole[25] has developed a "partial-mode" technique, which provides an experimental method of accounting for the sometimes important aerodynamic damping aspects of the problem. This method gets its name from the fact that only a part of the vehicle, and, consequently, only a part of the bending mode is simulated by the model. Using this technique, it was discovered that some configurations could have unstable aerodynamic damping. An example is shown in Fig. 18[25] where the usual stability notation aerodynamic damping coefficient $C_{m_q} + C_{m_{\dot{\alpha}}}$ is plotted as a function of Mach number for a particularly poor configuration. For this configuration, the aerodynamic damping becomes unstable at a Mach number of about 0.8 and remains unstable up to a Mach number of 1.0. Of course, the partial-mode technique does not account for aerodynamic damping or buffeting inputs on that part of the configuration which is not included in the model. On configurations such as the Saturn-Apollo there are significant areas of separation all the way to the base of the vehicle, and omission of their effect could lead to large discrepancies. In addition to this problem, the partial mode models are very closely coupled to the sting support, and extraneous sting modes sometimes lead to difficulty in interpreting the response data.

One technique, which tends to alleviate these problems, is the complete aeroelastically scaled model. Hanson and Doggett[26-29] have developed this approach following the successful application of this mechanical analog method to the airplane wing buffeting problem. Basically, this technique involves simulation of the complete vehicle as a beam with the beam supported on a sting by soft springs, which can be sized

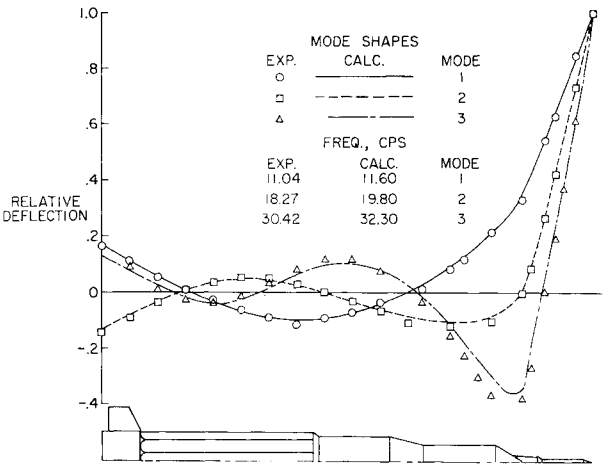

Fig. 19 Experimental and calculated natural frequencies for Apollo model configuration.

to give the model on the sting a rigid-body-pitch degree of freedom simulating that of the full-scale vehicle with its flight control system. Springs sized in this manner have been found to be sufficiently soft that they exert negligible influence on the free-free bending modes when they are attached to the model near the node points for the first mode. Mass and stiffness of the model beam are selected such that the model correctly simulates the reduced frequency and mass ratio of the full-scale vehicle at selected points on the trajectory.

The most recent of a series of these models was an 8% scale model of the Saturn-Apollo.[29] It was about 14.5 ft long and weighed about 760 lb. The degree to which this model simulated its design modes and frequencies is indicated in Fig. 19. Excellent agreement is indicated for the mode shapes through the third mode. Higher modes were obscured by extraneous shell modes of the model. The model frequencies were low by only about 5 to 8% of the design frequencies, which is considered adequate simulation.

Bending-moment response is measured at one or more stations on the model by simple strain-gage bridges, and the contributions of individual modes are scaled separately according to an uncoupled modal analysis[28] and recombined to give a predicted distribution of full-scale bending moments such as the example shown in Fig. 20. The "bumpy" behavior of the total bending-moment distribution is due to the significant contributions of the second and third modes. A similar procedure employing the strain-gage measurements of response could be employed to give predicted distributions of shear, deflection, acceleration, or any response quantity linearly related to displacement.

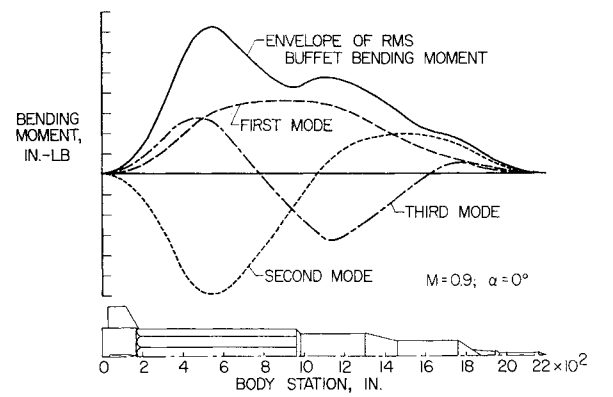

Fig. 20 Model contribution to buffet bending moment predicted from Saturn-Apollo model results.

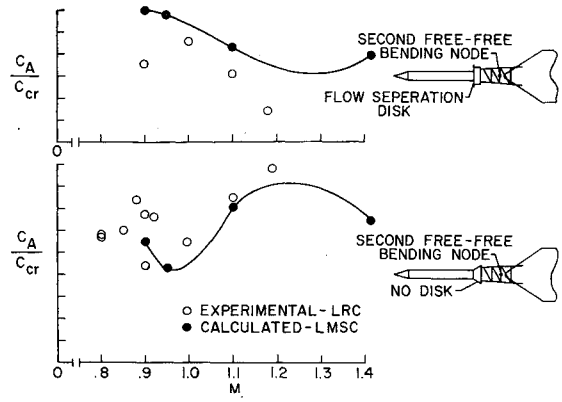

Fig. 21 Comparison of measured and calculated aerodynamic damping for Saturn-Apollo second bending mode.

Aerodynamic damping considerations

The complete aeroelastic model technique provides measurements of the aerodynamic damping obtained on the model which can be scaled directly to full-scale conditions. Aerodynamic damping coefficients were obtained for all three bending modes on the 8% scale Saturn-Apollo model for a variety of conditions, and the opportunity was taken to evaluate methods of calculating aerodynamic damping by direct comparison of calculated and measured results. One such interesting comparison is shown in Fig. 21. The calculated values shown in Fig. 21 are unpublished work of Lars-Eric Ericsson and J. P. Reding of Lockheed Missiles and Space Company employing a quasi-static technique using measured static aerodynamic derivatives.[30] Both the measured and calculated aerodynamic damping ratios are plotted as a function of Mach number and have been scaled to full-scale trajectory conditions. The cases shown in Fig. 21 were selected to illustrate the effect of a large flow separation disk which, at one time, was considered for use in the Apollo design. The results are presented for the second bending mode because the damping in this mode was particularly sensitive to the flow separator disk because of the location of the forward node point between the disk and the nose of the vehicle. Examination of Fig. 21 indicates an almost complete reversal of trend of aerodynamic damping with Mach number in the range from about 0.9 to 1.2 between the disk-on and disk-off cases. The measured and calculated results agree very well qualitatively in indicating this strong effect of the disk. The quantitative agreement is considered to be good in view of the experimental difficulty of measuring the small values of aerodynamic damping that launch vehicles experience and in view of the complexity of the aerodynamics which must be accounted for in making the calculation. The results shown in Fig. 21 are typical of other comparisons that have been made for variations of the basic Saturn-Apollo model, and it can be concluded that the quasi-static technique as developed by Ericsson and Reding will become a very useful tool in handling this aspect of the launch-vehicle buffeting problem.

Concluding Remarks

Progress achieved by the large number of investigators who have studied the launch-vehicle buffeting problem in the four years of its recognized existence has been reviewed. There remain many unanswered questions, particularly in the area of understanding the fundamental mechanisms of production of aerodynamic pressure fluctuations. However, progress in the technology required to engineer for buffeting has been substantial.

It was pointed out that buffeting pressures are dimensionally well behaved in that results obtained on wind-tunnel models, in most cases, can be scaled by reduced-frequency concepts to full-scale conditions. This dimensional behavior has led to a generalized spectrum of aerodynamically produced fluctuating pressure, which seems to indicate that some of the configuration dependency of buffeting pressures can be accounted for on dimensional grounds. A few measurements of space-time correlation characteristics for separated flows have become available which indicate a picture of convected, decaying patterns of pressure somewhat similar to that which has been found for attached boundary layers and jet noise.

The state of the art that has been presented for the high-frequency local response problem indicates a picture of developing techniques. This part of the buffeting problem is characterized by very complicated structural behavior of systems exposed to multiple random inputs, which are difficult to define. The approaches and methods for handling the problem exist, but they require further development and evaluation before it can be said that the problem is well in hand. Fortunately, a concerted effort is underway which should soon provide the technology required to make the various approaches suitable for general application in design.

The state of the art for the low-frequency bending response problem is in considerably better shape. The designer has a choice of several techniques, which appear to be well developed. Although these methods are basically experimental in nature, it was pointed out that a quasi-static prediction technique may be adequate in most cases for handling the aerodynamic damping aspects of this type of response.

References

[1] Coe, C. F., "Steady and fluctuating pressures at transonic speeds on two space-vehicle payload shapes," NASA TM X-503 (1961).

[2] Coe, C. F., "The effects of some variations in launch-vehicle nose shape on steady and fluctuating pressures at transonic speeds," NASA TM X-646 (1962).

[3] Coe, C. F. and Nute, J. B., "Steady and fluctuating pressures at transonic speeds on three 'hammerhead' launch vehicles," NASA TM X-778 (1962).

[4] Coe, C. F. and Kaskey, A. J., "The effects of nose cone angle and nose cone bluntness on the pressure fluctuation measured on cylindrical bodies at transonic speeds," NASA TM X-779 (1963).

[5] Goldberg, A. P. and Adams, R. H., "Mercury-Atlas buffeting loads at transonic speeds," Space Technology Labs., Inc., TR-60-0000-AS431 (November 1960).

[6] Jones, G. W., Jr. and Foughner, J. T., Jr., "Investigation of buffet pressures on models of large manned launch vehicle configurations," NASA TN D-1633 (1963).

[7] Chevalier, H. L. and Robertson, J. E., "Unsteady pressures and scale effects on models of the Titan B mark 4 re-entry body at transonic speeds," Arnold Engineering Development Center AEDC-TDR-62-178 (November 1962).

[8] Kelly, T. C., "Investigation at transonic Mach numbers of the effects of configuration geometry on surface pressure distributions for a simulated launch vehicle," NASA TM X-845 (1963).

[9] Robertson, J. E. and Chevalier, H. L., "Characteristics of steady-state pressures on the cylindrical portion of cone-cylinder bodies at transonic speeds," Arnold Engineering Development Center AEDC-TDR-63-104 (August 1963).

[10] Kistler, A. L., "The fluctuating wall pressures under a separated supersonic flow," Fluid Dynamics Panel of AGARD Specialists Meeting on the Mechanism of Noise Generation in Turbulent Flows, AGARD Rept. 458 (April 1963).

[11] Liepmann, H. W., "On the application of statistical concepts to the buffeting problem," J. Aeronaut. Sci. **19**, 793–800, 822 (1952).

[12] Liepmann, H. W., "Parameters for use in buffeting flight tests," Rept. SM-14631, Douglas Aircraft Co., Inc. (January 3, 1953).

[13] Peterson, H. C. and Ezra, A. A., "Analysis of similitude requirements and scaling laws for transonic buffeting," Proceedings of Symposium on Aeroelastic and Dynamic Modeling Technology, Part I, Paper RTD-TDR-63-4197, Research and Technology Div., Aerospace Industries Association (September 23–25, 1963).

[14] Willmarth, W. W. and Woolridge, C. E., "Measurements of the fluctuating pressure at the wall beneath a thick boundary layer," Univ. of Michigan, Dept. of Aeronautical and Astronautical Engineering, Technical Report (April 1962).

[15] Coe, C. F., "The effect of model scale on rigid-body unsteady pressures associated with buffeting," Proceedings of Symposium on Aeroelastic and Dynamic Modeling Technology, Part I, Paper RTD-TDR-63-4197, Research and Technology Div., Aerospace Industries Association (September 23–25, 1963).

[16] Henricks, W., "Flight test report for ranger vehicle 6005," Rept. SS/626/5351, Lockheed Missiles and Space Co./A384258 (1963).

[17] Houbolt, J. C., "On the response of structures having multiple random inputs," *Jahrbuch-1957 der Wissenschaftlichen Gesellschaft Fur Luftfahrt E. V. (WGL)* (Friedrich Vieweg and Sohn, Braunschweig, Germany), pp. 296–305.

[18] Goldberg, A. P. and Wood, J. D., "Dynamic loads in the Atlas-Able V during transonic buffeting," Space Technology Labs., Inc., TM-60-000-19075 (August 1960).

[19] Ezra, A. A. and Peterson, H. C., "Determination of design criteria for transonic buffeting forces acting on launch vehicles," ARS Preprint 2407-62 (April 1962).

[20] Peterson, H. C., "Dynamic response of launch vehicles to transonic buffeting forces," AIAA Preprint 63-209 (June 1963).

[21] Case, W., Stouffer, C. G., and Rowe, W. H., "Transonic local and integrated booster buffet loads on a 6.67% model of the 624A vehicle with X-20 and bulbous payloads," The Martin Co., ER 13024, Vol. I, Summary; Vol. II, Pressure Test; Vol. III, ICB Test (September 1963).

[22] Roberts, W. H., "Investigation of a method for the prediction of vibratory response and stress in typical flight vehicle structure," Aeronautical Systems Div. ASD-TDR-62-801 (August 1962).

[23] Roberts, W. H. and Walker, K., "Dynamic models for low cycle fatigue," Proceedings of Symposium on Aeroelastic and Dynamic Modeling Technology, Part I, Paper RTD-TDR-63-4197, Research and Technology Div., Aerospace Industries Association (September 23–25, 1963).

[24] Stahle, C. V., Stouffer, C. G., and Silver, W., "A simplified inertia-compensated balance technique for wind tunnel measurement of launch vehicle random buffet excitation," Proceedings of Symposium on Aeroelastic and Dynamic Modeling Technology, Part I, Paper RTD-TDR-63-4197, Research and Technology Div., Aerospace Industries Association (September 23–25, 1963).

[25] Cole, H. A., Jr. and Coe, C. F., "Dynamic response of Hammerhead launch vehicles to transonic buffering," NASA TN D-1982 (1963).

[26] Hanson, P. W. and Doggett, R. V., Jr., "Wind-tunnel measurements of aerodynamic damping derivatives of a launch vehicle vibrating in free-free bending modes at Mach numbers from 0.70 to 2.87 and comparisons with theory," NASA TN D-1391 (1962).

[27] Hanson, P. W. and Doggett, R. V., Jr., "Aerodynamic damping of a 0.02-scale Saturn SA-1 model vibrating in the first free-free bending mode," NASA TN D-1956 (1963).

[28] Doggett, R. V., Jr. and Hanson, P. W., "An aeroelastic model approach for the prediction of buffet bending loads on launch vehicles," NASA TN D-2022 (1963).

[29] Hanson, P. W. and Jones, G. W., Jr., "On the use of dynamic models for studying launch vehicle buffet and ground-wind loads," Proceedings of Symposium on Aeroelastic and Dynamic Modeling Technology, Part I, Paper RTD-TDR-63-4197, Research and Technology Div., Aerospace Industries Association (September 23–25, 1963).

[30] Ericsson, L.-E. and Reding, J. P., "Effects of various types of flow separation on launch vehicle dynamics," Eighth Symposium on Ballistic Missile and Space Technology (October 1963).